JOURNAL OF MATERIALS SCIENCE 21 (1986) 3223–3226

# X-ray analysis of microscopic structure in deformed brass

F. TUNG, S. ZWUI, Y. WANG
*Physics Department, Jilin University, Changchun 130023, China*

The microscopic structure of brass is systematically studied by X-ray diffraction profile analysis in this paper. The samples were heat treated differently and deformed in an unidirectional tensile state. Parameters such as the effective grain size, average dislocation density, dislocation configuration parameter and stored deformation energy density are carefully deduced from X-ray diffraction data based on some recent theories and models. These parameters change with macroscopic stress and strain regularly and it is possible to establish a quantitative relationship between the microscopic structure and macroscopic properties. There is an unique relationship between the structure parameters and stress rather than strain for different sample heat treatments.

## 1. Introduction

After plastic deformation in metals there are a lot of dislocations with various distributions regarding different degrees and ways of deformation [1]. Dislocations may be arranged to form subgrain boundaries or to cause a cell structure and thus make the coherent domain size smaller which can be evaluated by an X-ray method. In the case of dislocation pile-ups or random distribution there is a large long range strain field causing a specific broadening of X-ray diffraction profiles [2]. The macroscopic mechanical properties change correspondingly with the microscopic structure which can be studied statistically by X-ray diffraction. Line profile analysis is able to give the average coherent domain size, dislocation density and configuration. Stokes' [3] deconvolution method allows the separation of the physical broadening profiles from the instrumental ones and the Warren–Averbach [4, 5] analysis gives the domain size and mean square strain. Wilkens [6] has proposed a model of "restrictedly random" distribution of dislocations to analyse the line profiles and has obtained the dislocations density $\bar{\varrho}$, configuration parameter $\bar{M}$, strain field range $\bar{R}_e$ and stored elastic energy $(E/V)$ for monocrystal copper. Langford [7, 8] has suggested that each profile can be considered as a convolution of several Gaussian functions with Cauchy ones [7–9]. Based on the above mentioned ideas Wang *et al.* [10] has worked out a practical procedure and some standard curves for line profile analysis of fcc polycrystals. Recently satisfactory results have been obtained on hcp and bcc polycrystals and on multi-phase fcc alloys as well [11]. In this paper the results on commercial α-brass after unidirectional tensile deformation are presented.

## 2. Experimental details

Samples were cut from the commercial α-brass containing 31.55 wt % Zn, 0.6 mm thick, along the rolling direction. After polishing they were annealed in vacuum at two different temperatures for 2 h, namely at 617 K for samples of group A and at 651 K for those of group B. As for group C, samples of filings at room temperature without any annealing were used. Tensile deformation was performed at room temperature with a speed of 0.26 mm $min^{-1}$. The stress–strain curve is shown in Fig. 1.

X-ray diffraction line profiles were recorded by a rotating anode X-ray diffractometer with Cu$K\alpha$ radiation and a graphite monochromator. Two pairs of reflections 1 1 1/2 2 2 and 2 0 0/4 0 0 were measured on deformed and standard (annealed but not deformed) samples of 18 mm × 10 mm size.

After Stokes' [3] deconvolution the physical broadened profiles and its corresponding Fourier coefficients $A(L)$ were obtained and then the two components, "particle" coefficients $A^p(L)$ and "strain" coefficients $A^s(L)$ were separated according to [10] as

$$A^p(L) = a - \frac{L}{D_{eff}} \quad (1)$$

$$A^s(L) = \exp(-2\beta_0 L - \pi\beta_g^2 L^2) \quad (2)$$

where $a$ is the quantity expressing the "hook" effect, $L$ the specific length perpendicular to the reflecting planes, $D_{eff}$ the average "effective" coherent domain size, and $\beta_c$ and $\beta_g$ the Cauchy ad Gaussian widths of "strain" broadened profile, respectively. Making use of the standard curves and procedures described in [10], the average dislocation density $\bar{\varrho}$ and configuration parameter $\bar{M}$ have been obtained and they give directly the stored elastic energy density $E/V$

$$\frac{E}{V} = AG\bar{\varrho}b^2 \ln\frac{\bar{M}}{r_0(\varrho)^{1/2}} \quad (3)$$

where $A = 1/4\pi$ for screw dislocations, $A = 1/4\pi(1 - \nu)$ for edge dislocations, $\nu$ is Poissons ratio, $G$ is the shear modulus, $B$ is the dislocation strength and $r_0$ is the dislocation nucleus radius.

0022–2461/86 $03.00 + .12 

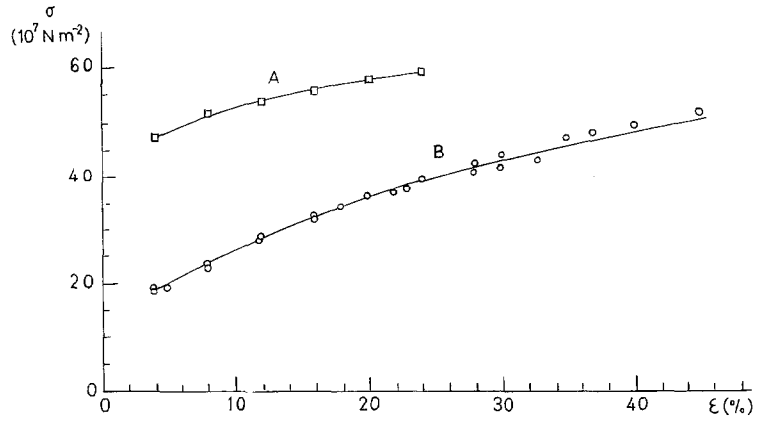


*Figure 1* Flow stress–strain curves for samples of group A and B. (□) Group A annealed at 617 K before deformation, (○) group B annealed at 615 K before deformation.

## 3. Results and discussion

The flow stress–strain curves for samples of group A and B are shown in Fig. 1. The data for both groups cannot be put on an unique curve, i.e. for a definite $\varepsilon$ there is big difference in $\sigma$ for samples annealed at different temperatures.

The $D_{\text{eff}}$–$\varepsilon$ curves are presented in Fig. 2 showing that $D_{\text{eff}}^{111}$ is always bigger than $D_{\text{eff}}^{200}$, especially after small deformation. At very severe deformation as in the case of filings, $D_{\text{eff}}^{111} \simeq D_{\text{eff}}^{200}$. The $D_{\text{eff}}$–$\varepsilon$ curves for samples of group B (experimental points in figures are expressed by small circles) are located higher than for samples of group A (experimental points in figures expressed by small squares). This is in correspondence with those in Fig. 1.

On the other hand, Fig. 3 shows the $D_{\text{eff}}$–$\sigma$ relationships which can be expressed by an unique curve for samples of both groups, i.e. there is a one to one correspondence between $D_{\text{eff}}$ and $\sigma$ in spite of the history of sample treatments. So it might be possible in the future to evaluate flow stress by only measuring microstructural parameters such as $D_{\text{eff}}$ and others without destroying the sample.

In Fig. 4, $(E/V)$ is calculated by Equation 3 as follows. Supposing the 1 1 1 reflection is affected only by screw dislocations, one can obtain $(E/V)_s^{111}$. Then $(E/V)_e^{111}$, $(E/V)_s^{222}$ and $(E/V)_e^{222}$ can also be deduced in the same way, where the subscript e or s denotes the edge or screw type of dislocations, respectively. A crude average is made as

$$\left(\frac{E}{V}\right)^{111} = \frac{1}{4}\left[\left(\frac{E}{V}\right)_s^{111} + \left(\frac{E}{V}\right)_e^{111} + \left(\frac{E}{V}\right)_s^{222} + \left(\frac{E}{V}\right)_e^{222}\right] \quad (4)$$

and similarly the $(E/V)^{200}$. It is clearly shown in Fig. 4 that $(E/V)^{111}$ is always smaller than $(E/V)^{200}$ and the difference increases rapidly with increasing deformation.

Comparing Fig. 4 with Fig. 2, one can notice that at $\varepsilon < 12\%$ the deformation work is mainly used to destroy the original crystal grains while after $\varepsilon > 18\%$ the energy stored inside the domain increases rapidly because of the increasing dislocation density. The $(E/V)$–$\varepsilon$ curve for group B is lower than that for group A, in correspondence with those in Figs 1 and 2. One should keep in mind that $(E/V)$ obtained by us from Equation 4 is not a precise average. In order to improve it the weighted average of real screw and edge dislocation densities and configuration parameters have to be considered.

From Fig. 5 one can seen that data for both A and B group of samples again may be put on one unique $(E/V)$–$\sigma$ curve unlike the case of $(E/V)$–$\varepsilon$ curves.

It is clear in Fig. 6, dislocation density at first increases with increasing $\varepsilon$ but stops changing at $\bar{\varrho} > 10^{10}\,\text{cm}^{-2}$, while $\bar{M}$ rapidly reduces at large deformations, especially for $\bar{M}$ (2 0 0/4 0 0). This probably means that dislocations exist mainly in pile-ups at small deformation to form a long range strain field while with increasing deformation the dislocations will gradually form the regular lattice of dipoles or rows normal to the glide plane and the long range strains cancel each other out.

There is significant difference in the above stated structural parameters between those deduced from 1 1 1/2 2 2 and from 2 0 0/4 0 0. For our plate sample, any $h\,k\,l$ reflection is given by those crystal grains whose $\{h\,k\,l\}$ planes are parallel to the sample surface. Different reflections are attributed to grains of different orientations which certainly have different

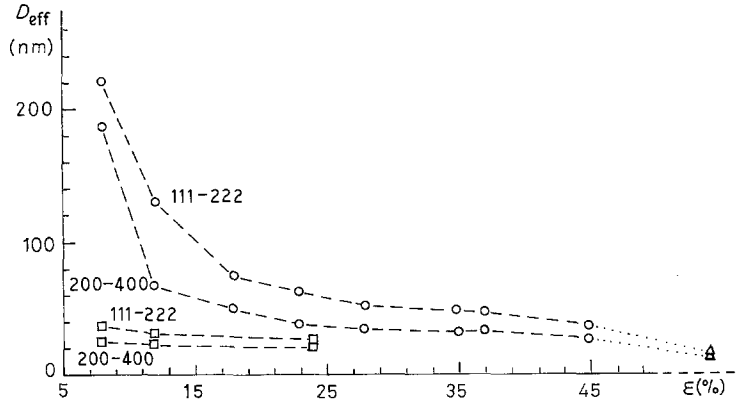


*Figure 2* Effective domain size against strain curves for samples of group A, B and C (□) group A, (○) group B, (△) group C (filings).

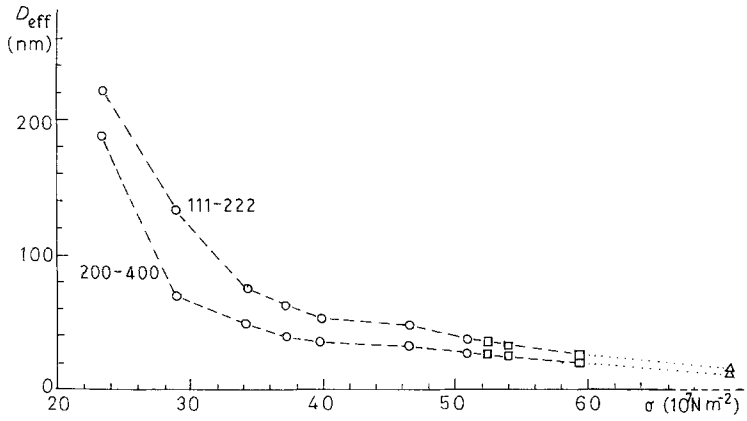


*Figure 3* Effective domain size against flow stress curves. (○) 111–222, (□) 200–400.

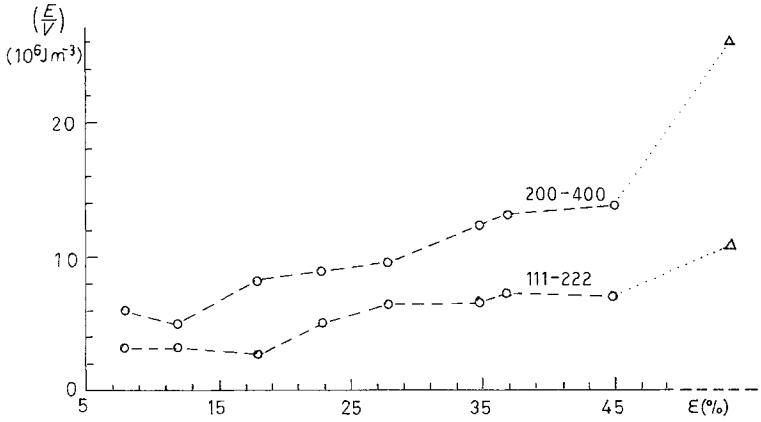


*Figure 4* Average stored energy density against strain curves.

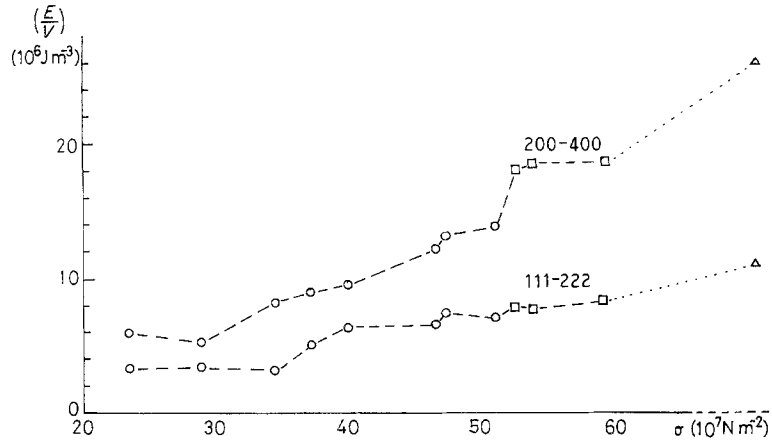


*Figure 5* Average stored energy density against flow stress curves.

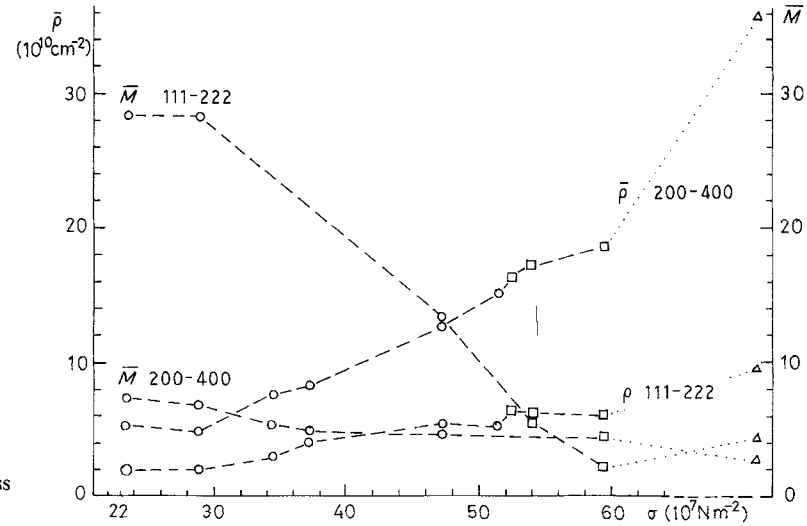


*Figure 6* Dislocation parameters against flow stress curves.

stress and strain states hence different structural parameters.

The data obtained from the filings are put together on the curves in Figs 2 to 5 with those of tensile samples to show the reasonable tendency of curves. But our data for filings are a little different from others [12, 13].

## 4. Conclusions

The X-ray method for studying a deformed structure is a non-destructive one which can give the statistically averaged microscopic parameters associated uniquely with the macroscopic flow stress regardless of the heat treatment history of the sample. This may allow a prediction of the macroscopic properties from the microscopic structure.

The quantitative relationship between macroscopic mechanical properties and the microscopic deformed structure could probably improve the work-hardening theory for metals.

## References


1. P. HAASEN, in "Physical Metallurgy" (Cambridge University Press, Cambridge, 1978) p. 243.
2. H. P. KLUG, in "X-ray Diffraction Procedures" (Wiley, New York, 1974) p. 618.
3. A. R. STOKES, *Proc. Phys. Soc.* **61** (1948) 382.
4. B. E. WARREN, in "Progress in Metal Physics" (Pergamon Press, London, 1959) p. 147.
5. *Idem*, "X-ray Diffraction" (Addison-Wesley, Reading, Massachusetts, 1969) p. 251.
6. M. WILKENS, *Phys. Status Solidi A* **21** (1970) 359.
7. J. I. LANGFORD, *J. Appl. Cryst.* **11** (1978) 10.
8. J. I. LANGFORD and A. J. C. WILSON, in "Crystallography and Crystal Perfections" (Academic Press, New York, 1963) p. 207.
9. J. M. COWLEY, in "Diffraction Physics" (North-Holland, Amsterdam, 1975) p. 25.
10. WANG YUMING, LEE SHANSAN and LEE YEN-CHIN, *J. Appl. Cryst.* **15** (1982) 35.
11. S. ZWUI, *J. Mater. Sci. Lett.* **4** (1985) 1434.
12. J. B. COHEN and J. E. HILLIARD, in "Local Atomic Arrangement Studied by X-ray Diffraction" (Gordon Breach, New York, 1965) p. 289.
13. E. MAGEE and W. J. KITCHINGMAN, *J. Phys. D: Appl. Phys.* **9** (1976) 939.



*Received 19 September*
*and accepted 30 October 1985*